ICHEP94 Ref. GLS0460 **CLEO CONF 94-23**
Submitted to PA 16 Pl 9 **July 19, 1994**

Study of the decays $\tau^- \to K^0_S h^- (\pi^0) \nu_\tau$

M. Athanas,[1] W. Brower,[1] G. Masek,[1] H.P. Paar,[1] M. Sivertz,[1] J. Gronberg,[2] R. Kutschke,[2] S. Menary,[2] R.J. Morrison,[2] S. Nakanishi,[2] H.N. Nelson,[2] T.K. Nelson,[2] C. Qiao,[2] J.D. Richman,[2] A. Ryd,[2] H. Tajima,[2] D. Sperka,[2] M.S. Witherell,[2] R. Balest,[3] K. Cho,[3] W.T. Ford,[3] D.R. Johnson,[3] K. Lingel,[3] M. Lohner,[3] P. Rankin,[3] J.G. Smith,[3] J.P. Alexander,[4] C. Bebek,[4] K. Berkelman,[4] K. Bloom,[4] T.E. Browder,[4*] D.G. Cassel,[4] H.A. Cho,[4] D.M. Coffman,[4] D.S. Crowcroft,[4] P.S. Drell,[4] D. Dumas,[4] R. Ehrlich,[4] P. Gaidarev,[4] R.S. Galik,[4] M. Garcia-Sciveres,[4] B. Geiser,[4] B. Gittelman,[4] S.W. Gray,[4] D.L. Hartill,[4] B.K. Heltsley,[4] S. Henderson,[4] C.D. Jones,[4] S.L. Jones,[4] J. Kandaswamy,[4] N. Katayama,[4] P.C. Kim,[4] D.L. Kreinick,[4] G.S. Ludwig,[4] J. Masui,[4] J. Mevissen,[4] N.B. Mistry,[4] C.R. Ng,[4] E. Nordberg,[4] J.R. Patterson,[4] D. Peterson,[4] D. Riley,[4] S. Salman,[4] M. Sapper,[4] F. Würthwein,[4] P. Avery,[5] A. Freyberger,[5] J. Rodriguez,[5] S. Yang,[5] J. Yelton,[5] D. Cinabro,[6] T. Liu,[6] M. Saulnier,[6] R. Wilson,[6] H. Yamamoto,[6] T. Bergfeld,[7] B.I. Eisenstein,[7] G. Gollin,[7] B. Ong,[7] M. Palmer,[7] M. Selen,[7] J. J. Thaler,[7] K.W. Edwards,[8] M. Ogg,[8] A. Bellerive,[9] D.I. Britton,[9] E.R.F. Hyatt,[9] D.B. MacFarlane,[9] P.M. Patel,[9] B. Spaan,[9] A.J. Sadoff,[10] R. Ammar,[11] P. Baringer,[11] A. Bean,[11] D. Besson,[11] D. Coppage,[11] N. Copty,[11] R. Davis,[11] N. Hancock,[11] M. Kelly,[11] S. Kotov,[11] I. Kravchenko,[11] N. Kwak,[11] H. Lam,[11] Y. Kubota,[12] M. Lattery,[12] M. Momayezi,[12] J.K. Nelson,[12] S. Patton,[12] R. Poling,[12] V. Savinov,[12] S. Schrenk,[12] R. Wang,[12] M.S. Alam,[13] I.J. Kim,[13] Z. Ling,[13] A.H. Mahmood,[13] J.J. O'Neill,[13] H. Severini,[13] C.R. Sun,[13] F. Wappler,[13] G. Crawford,[14] C. M. Daubenmier,[14] R. Fulton,[14] D. Fujino,[14] K.K. Gan,[14] K. Honscheid,[14] H. Kagan,[14] R. Kass,[14] J. Lee,[14] R. Malchow,[14] Y. Skovpen,[14†] M. Sung,[14] C. White,[14] M.M. Zoeller,[14] F. Butler,[15] X. Fu,[15] B. Nemati,[15] W.R. Ross,[15] P. Skubic,[15] M. Wood,[15] M. Bishai,[16] J. Fast,[16] E. Gerndt,[16] R.L. McIlwain,[16] T. Miao,[16] D.H. Miller,[16] M. Modesitt,[16] D. Payne,[16] E.I. Shibata,[16] I.P.J. Shipsey,[16] P.N. Wang,[16] M. Battle,[17] J. Ernst,[17] L. Gibbons,[17] Y. Kwon,[17] S. Roberts,[17] E.H. Thorndike,[17] C.H. Wang,[17] J. Dominick,[18] M. Lambrecht,[18] S. Sanghera,[18] V. Shelkov,[18] T. Skwarnicki,[18] R. Stroynowski,[18] I. Volobouev,[18] G. Wei,[18] P. Zadorozhny,[18] M. Artuso,[19] M. Gao,[19] M. Goldberg,[19] D. He,[19] N. Horwitz,[19] G.C. Moneti,[19] R. Mountain,[19] F. Muheim,[19] Y. Mukhin,[19] S. Playfer,[19] Y. Rozen,[19] S. Stone,[19] X. Xing,[19] G. Zhu,[19] J. Bartelt,[20] S.E. Csorna,[20] Z. Egyed,[20] V. Jain,[20] D. Gibaut,[21] K. Kinoshita,[21] P. Pomianowski,[21] B. Barish,[22] M. Chadha,[22] S. Chan,[22] D.F. Cowen,[22] G. Eigen,[22] J.S. Miller,[22] C. O'Grady,[22] J. Urheim,[22] and A.J. Weinstein[22]

(CLEO Collaboration)

[1] *University of California, San Diego, La Jolla, California 92093*
[2] *University of California, Santa Barbara, California 93106*
[3] *University of Colorado, Boulder, Colorado 80309-0390*
[4] *Cornell University, Ithaca, New York 14853*
[5] *University of Florida, Gainesville, Florida 32611*
[6] *Harvard University, Cambridge, Massachusetts 02138*
[7] *University of Illinois, Champaign-Urbana, Illinois, 61801*
[8] *Carleton University, Ottawa, Ontario K1S 5B6 and the Institute of Particle Physics, Canada*
[9] *McGill University, Montréal, Québec H3A 2T8 and the Institute of Particle Physics, Canada*
[10] *Ithaca College, Ithaca, New York 14850*
[11] *University of Kansas, Lawrence, Kansas 66045*
[12] *University of Minnesota, Minneapolis, Minnesota 55455*
[13] *State University of New York at Albany, Albany, New York 12222*
[14] *Ohio State University, Columbus, Ohio, 43210*
[15] *University of Oklahoma, Norman, Oklahoma 73019*
[16] *Purdue University, West Lafayette, Indiana 47907*
[17] *University of Rochester, Rochester, New York 14627*
[18] *Southern Methodist University, Dallas, Texas 75275*
[19] *Syracuse University, Syracuse, New York 13244*
[20] *Vanderbilt University, Nashville, Tennessee 37235*
[21] *Virginia Polytechnic Institute and State University, Blacksburg, Virginia, 24061*
[22] *California Institute of Technology, Pasadena, California 91125*

Abstract

Using the large $\tau^+\tau^-$ data sample taken with the CLEO II detector at the CESR e^+e^- collider, we study the decays $\tau^- \to K^0_S h^- \nu_\tau$ and $\tau^- \to K^0_S h^- \pi^0 \nu_\tau$, where h^- may be a pion or a kaon. Preliminary branching fractions are determined to be $\mathcal{B}(\tau^- \to \overline{K}^0 h^- \nu_\tau) = (0.977 \pm 0.023 \pm 0.108)\%$ and $\mathcal{B}(\tau^- \to \overline{K}^0 h^- \pi^0 \nu_\tau) = (0.519 \pm 0.035 \pm 0.062)\%$. We also study the mass spectra and, in the $K^0_S h^- \pi^0$ system, the contributions from $K_1(1270)$ and $K_1(1400)$.

[*] Permanent address: University of Hawaii at Manoa

[†] Permanent address: INP, Novosibirsk, Russia

I. INTRODUCTION

Decays of the τ lepton provide a potentially powerful probe of the strange sector of the weak charged current. Previous experimental results [1] have been limited by low statistics and/or poor kaon identification capability, although the situation has improved in the last two years [2–5]. The CLEO detector has accumulated a large sample of e^+e^- data in the center of mass energy (E_{cm}) region near 10.6 GeV. We have recently published a study of Cabibbo suppressed τ decay [6] using identified charged kaons. This analysis makes use of τ decay final states containing a $K_S^0 \to \pi^+\pi^-$ decay, which can be identified unambiguously and with little background. The final states under study also contain a charged hadron [7] h^- and potentially a π^0. In this paper we make no attempt at π/K identification of the h^-, but we expect [2] these final states to be dominated by $\tau^- \to K_S^0\pi^-(\pi^0)\nu_\tau$. In companion contributions to this conference [8] [9], we also study the final states to KK and $KK\pi$.

In τ decay, strange ($\overline{u}s$) currents are suppressed relative to the non-strange ($\overline{u}d$) currents by the ratio of Kobayashi-Maskawa matrix elements $|V_{us}/V_{ud}|^2 \approx \tan^2\theta_C$, where θ_C is the Cabibbo angle. In analogy with the non-strange currents, both the vector and axial-vector components of the strange current are expected [1] to be dominated by resonances: the vector current by the K^* resonance, which decays to $K\pi$, and the axial-vector current by the K_1 resonances, decaying predominantly through $K\rho$ and $K^*\pi$ to $K\pi\pi$. The spectral functions describing these decays can be related, via the Das-Mathur-Okubo (DMO) sum rules [10], to the non-strange currents. For example, if the non-strange and strange vector currents are both dominated by the single resonances ρ and K^*, respectively, and if the narrow-width approximation is used, then the DMO sum rule gives $f_{K^*}/M_{K^*} = f_\rho/M_\rho$, where M and f are the mass and vector decay constant of the corresponding mesons, respectively.

In the axial-vector current, there are two $\overline{u}d$ ($\overline{u}s$) states with similar masses: the $^3P_1$ and $^1P_1$ states, corresponding to $a_1(1260)$ (K_{1A}) and $b_1(1235)$ (K_{1B}), respectively. In the case of $\overline{u}d$, the production of $b_1(1235)$ from τ decays proceeds through a second-class current, which is highly suppressed due to isospin symmetry; only the $a_1(1260)$ has been observed [11]. In the corresponding $\overline{u}s$ case, second-class currents are suppressed only by $SU(3)_f$ symmetry, which is broken by the large strange quark mass. Thus, we expect some K_{1B} production from τ decays along with K_{1A}, and their relative amount is a measure of $SU(3)_f$ symmetry breaking [12]. However, the observed resonances [11], denoted by $K_1(1270)$ (which decays mainly to $K\rho$) and $K_1(1400)$ (decaying mainly to $K^*\pi$), are believed to be a mixture of K_{1A} and K_{1B} [13], parameterized by a mixing angle θ_K. Hence, a determination of the τ decay rates to $K_1(1270)$ and $K_1(1400)$, along with an analysis of the resonant substructure in these decays, will allow us to probe both the $SU(3)_f$ symmetry breaking and the K_{1A} – K_{1B} mixing. One can also determine if there is any non-resonant $K\pi\pi$ production in τ decay.

II. ANALYSIS

The data were accumulated by the CLEO II detector with the CESR e^+e^- collider. The detector is described in detail elsewhere [14]. The analysis uses information from a 67-layer tracking system and a 7800-crystal CsI calorimeter, both of which are inside a 1.5 T superconducting solenoid, and a muon identification system. A total integrated luminosity of 2.962 fb^{-1} is used for this analysis, corresponding to a total number of produced tau pairs, $N_{\tau\tau} = (2.707 \pm 0.038) \times 10^6$. The results of the data analysis are compared with a Monte Carlo simulation of $\tau^+\tau^-$ production and decay [15], and a full GEANT-based detector simulation [16]. We simulate the $\tau^- \to K\pi\pi\nu_\tau$ decay process using a model based on chiral perturbation theory [17].

We select events containing exactly four charged tracks with momentum transverse to the beam $P_t > 0.1$ GeV/c and $|\cos\theta| < 0.9$ (where θ is the angle between the track and the beam axis), with net charge zero. One track must be isolated from the other three by at least 90°, dividing the event into a 1-prong *vs.* 3-prong topology. The track on the 1-prong side is identified as either an e^+, μ^+, h^+, or $h^+\pi^0$ (if the track is accompanied by photons in the calorimeter consistent with $\pi^0 \to \gamma\gamma$). All such assignments are used to tag the $\tau^+\tau^-$ event, and the breakdown by tag type is used as a cross-check on the analysis. Cuts are applied to the total visible energy and total visible transverse momentum of the event (both charged tracks and calorimeter showers are included), to suppress non-$\tau^+\tau^-$ backgrounds. An event is vetoed if it contains photon-like showers not associated with a reconstructed π^0 ($>$ 100(250) MeV for $|\cos\theta| < 0.71(0.95)$), or if there are any showers with energy $>$ 350 MeV unassociated with a π^0.

Pairs of calorimeter showers on the 3-prong side are combined to form π^0 candidates. The pair invariant mass must be within three standard deviations of the π^0 mass: $|S_{\gamma\gamma}| < 3$, with $S_{\gamma\gamma} \equiv (M_{\gamma\gamma} - M_{\pi^0})/\sigma_{\gamma\gamma}$. The expected value of $\sigma_{\gamma\gamma}$ is evaluated for each photon pair, and is typically 5-8 MeV/c^2 for $\pi^0 \to \gamma\gamma$.

A $K^0_S \to \pi^+\pi^-$ decay is identified in the 3-prong side of the event by reconstructing two-track vertices which are separated from the event primary vertex by 5 mm in the plane perpendicular to the beam axis. A variety of cuts are made to ensure that the secondary vertex is of good quality and inconsistent with coming from a photon pair conversion. The $M_{\pi\pi}$ distribution for $\tau^- \to K^0_S h^-\nu_\tau$ candidates, and the $M_{\pi\pi}$ *vs.* $S_{\gamma\gamma}$ distributions for $K^0_S h^-\pi^0\nu_\tau$ candidates, are shown in Fig. 1. The resulting K^0_S lifetime distribution (Fig. 2) is in good agreement with Monte Carlo expectations.

III. BACKGROUNDS AND EFFICIENCY

Backgrounds from events not containing K^0_S decays (not containing K^0_S-π^0 in $K^0_S h^-\pi^0$ mode) are statistically subtracted by means of a sideband technique. The sideband regions are illustrated in Fig. 1.

Based on studies of the global kinematic properties of the events as compared with Monte Carlo predictions, there is no evidence for $B\overline{B}$, or e^+e^-X two-photon production backgrounds. We estimate from Monte Carlo that there is a background of 51.6 ± 13.3 events in the $K^0_S h^-$ sample and 24.7 ± 10.8 events in the $K^0_S h^-\pi^0$ sample. Uncertainties in these estimates contribute to the systematic errors on the branching fractions.

Monte Carlo is used to estimate backgrounds from $\tau^+\tau^-$ events. The main sources of such backgrounds are from events containing an unobserved K^0_L or π^0. In subtracting the background from $K^0 h^-\pi^0\nu_\tau$ and $K^0\overline{K^0}\pi^-\nu_\tau$, we use branching ratios found in this study and in the companion contribution [9].

Monte Carlo is used to determine the efficiency. Two different methods are used. In the first, data and Monte Carlo events satisfying all cuts are counted, assuming that the mass spectrum of the signal is well modeled in the Monte Carlo. The efficiency is calculated separately for each tag decay mode. In the second, the efficiency is calculated in $M(K_S^0 h^-(\pi^0))$ mass bins, and the resulting distribution is fitted to a polynomial curve. This latter method is also used to find both the branching fraction and the efficiency-corrected mass distribution, suitable for spectral function studies.

IV. RESULTS

We find 2307 events in the $K_S^0 h^-$ mode and 443 events in the $K_S^0 h^- \pi^0$ mode. The invariant mass distributions for these two samples are shown in Figs. 3 and 4, respectively. Also shown are Monte Carlo predictions for the various background contributions. In both distributions, the number of events with $M(K_S^0 h^-(\pi^0)) > M_\tau$ is small and consistent with background estimations.

The branching ratios are determined by the following formula:

$$\mathcal{B}(\text{signal}) = \frac{N(1 - f_b^{qq} - f_b^{\tau\tau})}{2N_{\tau\tau} \sum_j \mathcal{B}_j \mathcal{E}_j}, \tag{1}$$

where N is the number of events observed (after sideband subtraction), $f_b^{\tau\tau}$ is the background fraction from $\tau^+\tau^-$ sources, f_b^{qq} is the background fraction from non-$\tau^+\tau^-$ sources, $N_{\tau\tau}$ is the number of produced $\tau^+\tau^-$ events, $\mathcal{B}_j$ is the branching ratio for tag j (from [2]), and $\mathcal{E}_j$ is the efficiency for observing the signal with tag j (determined using Monte Carlo). When mass dependent efficiencies are used, Eqn. 1 is generalized in a straightforward way.

The values of the quantities in Eqn. 1, along with their estimated errors, are summarized in Table I. We find

$$\mathcal{B}(\tau^- \to \overline{K}^0 h^- \nu_\tau) = (0.977 \pm 0.023 \pm 0.108)\%, \tag{2}$$
$$\mathcal{B}(\tau^- \to \overline{K}^0 h^- \pi^0 \nu_\tau) = (0.519 \pm 0.035 \pm 0.062)\%, \tag{3}$$

where the first errors are statistical and the second systematic.

Contributions to the systematic errors from a variety of sources are itemized in Table II. Since the studies are still underway, we are conservative in assigning the systematic errors. The errors will certainly decrease after more detailed studies are finished.

The systematic error associated with the total number of $\tau^+\tau^-$ events, $N_{\tau\tau}$, is due to the uncertainties in the luminosity determination (1%) and the $\tau^+\tau^-$ cross-section (1%). For the non-τ background, 100% systematic error on f_b^{qq} is assigned based on varying the corresponding cuts. The error on τ background comes partly from the uncertainty in input branching ratios and partly from the error in detection probability of the backgrounds. As a cross-check, we have separated the event sample according to the individual tag decay modes and have computed the $\tau^- \to K_S^0 h^-(\pi^0)$ branching ratios for each of them. Based on the deviations of these results, we assign systematic errors on the overall branching ratios to account for possible additional errors in background or efficiency estimation in the tag hemisphere. There is good agreement between the event counting and the efficiency-corrected mass distribution methods. The distributions of a wide variety of kinematic and detector-dependent variables agree well between data and Monte Carlo, including the mass distributions presented in the next section.

TABLE I. Quantities entering into branching fraction determinations for the $K_S^0 h^-$ and $K_S^0 h^- \pi^0$ modes.

Mode	Quantity	Value	σ_{stat}	σ_{syst}	$\sigma(\mathcal{B})/\mathcal{B}$
	N	2307	55	—	2.4%
	f_b^{qq}	0.022	—	0.022	2.7%
	$f_b^{\tau\tau}$	0.138	—	—	5.4%
$K_S^0 h^-$	$N_{\tau\tau}$	2707000	—	38000	1.4%
	$\sum_j \mathcal{B}_j \mathcal{E}_j$	0.107	—	—	9.2%
	$\mathcal{B}(\tau^- \to \overline{K}^0 h^- \nu_\tau)$	0.977%	0.023%	0.108%	—
	N	443	30	—	6.8%
	f_b^{qq}	0.056	—	0.0557	6.3%
	$f_b^{\tau\tau}$	0.060	—	—	4.6%
$K_S^0 h^- \pi^0$	$N_{\tau\tau}$	2707000	—	38000	1.4%
	$\sum_j \mathcal{B}_j \mathcal{E}_j$	0.041	—	—	9.2%
	$\mathcal{B}(\tau^- \to \overline{K}^0 h^- \pi^0 \nu_\tau)$	0.519%	0.035%	0.062%	—

TABLE II. Systematic errors on branching ratios, $\sigma(\mathcal{B})/\mathcal{B}$.

Quantity	Category	$K_S^0 h^- \nu_\tau (\%)$	$K_S^0 h^- \pi^0 \nu_\tau (\%)$
$N_{\tau\tau}$	$N_{\tau\tau}$	1.4	1.4
f_b^{qq}	Non-τ background	2.7	6.3
$f_b^{\tau\tau}$	τ background	4.5	3.5
$f_b^{\tau\tau}$	γ veto	3.0	3.0
$\mathcal{B}\mathcal{E}$	Tracking	5.1	5.1
$\mathcal{B}\mathcal{E}$	K_S^0 finding	5.0	5.0
$\mathcal{B}\mathcal{E}$	π^0 finding	—	3.0
$\mathcal{B}\mathcal{E}$	Signal extraction (sideband)	3.0	4.0
$\mathcal{B}\mathcal{E}$	Tag dependency	5.0	3.0

V. MASS DISTRIBUTIONS

The invariant mass distributions of the $K^0_S h^-$ and the $K^0_S h^- \pi^0$ system for the sideband-subtracted and background-subtracted signals are plotted in Fig. 5 and Fig. 6, respectively. The π^- mass is assigned to all three charged tracks. The momentum of each charged track is corrected for dE/dx energy loss in the detector. The energies and directions of the photons from the π^0 candidate (in the $K^0_S h^- \pi^0$ mode) are modified, within their error, to constrain $M_{\gamma\gamma}$ to be M_{π^0}.

The histograms in Figs. 5 and 6 are the results of fits to the background-subtracted data with Monte Carlo predicted contributions from the sources indicated in the figures. The mass spectra and relative contributions from $K^0_S K^- / K^0_S K^- \pi^0$ are taken from results obtained in a parallel analysis of those final states [8].

In the $K^0_S h^-$ mode (Fig. 5), a contribution from $K^0_S K^-$ describes the enhancement above the K^* peak well. There is no evidence for a non-resonant $K^0_S \pi^-$ contribution.

In the $K^0_S h^- \pi^0$ mode (Fig. 6), the data is well described by an incoherent sum of contributions from the $K_1(1270)$, $K_1(1400)$ and $K^0_S K^- \pi^0$. In contrast to a previous measurement [5] indicating that τ decays preferentially proceed through $K_1(1400)$ rather than $K_1(1270)$, our fit suggests that $K_1(1270)$ dominates over $K_1(1400)$.

An understanding of $SU(3)_f$ symmetry breaking and $K_{1A} - K_{1B}$ mixing requires a study of the resonant substructure in the two mass regions. We show in Fig. 7 the Dalitz plots for the $M(K^0_S \pi^- \pi^0)$ mass regions around 1270 MeV/c^2 and 1400 MeV/c^2, for both data and Monte Carlo. In both cases, the contribution from $K^0_S K^- \pi^0$ is included. The rates assumed for the K_1 decays to $K\rho$ and $K^*\pi$ in the Monte Carlo come from Ref. [11]. Detailed fits to these distributions as a function of $M(K^0_S \pi^- \pi^0)$ are in progress.

VI. SUMMARY AND DISCUSSION

In conclusion, we present preliminary measurements of the τ lepton to the final states $K^0_S h^- \nu_\tau$ and $K^0_S h^- \pi^0 \nu_\tau$ to be:

$$\mathcal{B}(\tau^- \to \overline{K}^0 h^- \nu_\tau) = (0.977 \pm 0.023 \pm 0.108)\%,$$
$$\mathcal{B}(\tau^- \to \overline{K}^0 h^- \pi^0 \nu_\tau) = (0.519 \pm 0.035 \pm 0.062)\%,$$

using 2.962 fb^{-1} of CLEO II data where the K^0 is detected through $K^0_S \to \pi^+\pi^-$. The statistical errors are considerably smaller than those from previous measurements. We can combine the results and obtain $\mathcal{B}(\tau^- \to \overline{K}^0 h^- n\pi^0 \nu_\tau, n = 0, 1) = (1.50 \pm 0.04 \pm 0.16)\%$.

We have previously measured [6] $\mathcal{B}(\tau^- \to K^- \pi^0 \nu_\tau)$ to be $(0.51 \pm 0.10 \pm 0.07)\%$. For comparison, we subtract the measurement $\mathcal{B}(\tau^- \to K^0 K^- \nu_\tau) = (0.123 \pm 0.023 \pm 0.023)\%$ [8] from $\mathcal{B}(\tau^- \to K^0 h^- \nu_\tau)$ to obtain $\mathcal{B}(\tau^- \to \overline{K}^0 \pi^- \nu_\tau) = (0.85 \pm 0.03 \pm 0.11)\%$. This is in good agreement with the isospin prediction that this branching fraction should be twice that of $\tau^- \to K^- \pi^0 \nu_\tau$. This result also agrees with the recent ALEPH result of $\mathcal{B}(\tau^- \to \overline{K}^0 \pi^- \nu_\tau)$ $= (0.88 \pm 0.14 \pm 0.09)\%$ [4].

As a test of the DMO sum rule, we assume that the $\tau^- \to \overline{K}^0 \pi^- \nu_\tau$ rate is saturated by the K^{*-} resonance. Using isospin, we use our value of $\overline{K}^0 \pi^- \nu_\tau$ to determine an expected value for $K^-\pi^0\nu_\tau$, which we subtract from our recent measurement of $\mathcal{B}(\tau^- \to h^-\pi^0\nu_\tau) = (25.87 \pm 0.12 \pm 0.42)\%$ [18], to obtain the $\pi^-\pi^0\nu_\tau$ rate. We assume it to be saturated by ρ^- resonance. The presence of a ρ' contribution in the $\tau \to \pi\pi\nu_\tau$ decay [18] distorts the $M_{\pi\pi}$ mass distribution but does not significantly change the branching fraction, so we do not correct for it. Taking the ratio of Kobayashi-Maskawa matrix elements from Ref. [11], we obtain

$$\frac{|V_{ud}|^2}{|V_{us}|^2}\frac{\mathcal{B}(\tau^- \to K^{*-}\nu_\tau)}{\mathcal{B}(\tau^- \to \rho^-\nu_\tau)} = 0.98 \pm 0.03 \pm 0.13. \tag{4}$$

The prediction from the DMO sum rule (under the narrow-width, single-resonance assumptions) is 0.93. More detailed tests of the DMO sum rule require the extraction of the spectral functions; this work is in progress.

The $K_S^0h^-\pi^0\nu_\tau$ mass distribution shows evidence for both $\tau^- \to K_1^-(1270)\nu_\tau$ and $K_1^-(1400)\nu_\tau$. Further study of the $K_S^0\pi^-\pi^0$ system is in progress.

VII. ACKNOWLEDGMENTS

We gratefully acknowledge the effort of the CESR staff in providing us with excellent luminosity and running conditions. This work was supported by the National Science Foundation, the U.S. Dept. of Energy, the Heisenberg Foundation, the SSC Fellowship program of TNRLC, Natural Sciences and Engineering Research Council of Canada, and the A.P. Sloan Foundation.

REFERENCES

[1] M. T. Ronan, published in *The Proceedings of the Second Workshop on Tau Lepton Physics* , Columbus OH, September 1992, ed. K.K. Gan, World Scientific, 1993.

[2] A. Schwarz, published in *The Proceedings of the XVI International Symposium on Lepton Photon Interactions*, Cornell University, August 1993, ed. P. Drell and D. Rubin, AIP Press, 1994.

[3] ALEPH Collaboration (D. Buskulic, *et al.*), CERN-PPE-94-058, Apr 1994.

[4] ALEPH Collaboration (D. Buskulic, *et al.*), CERN-PPE-94-059, Apr 1994.

[5] TPC/2γ Collaboration (D. A. Bauer *et al.*), *Phys. Rev.* **D50**, R13 (1994).

[6] CLEO Collaboration (M. Battle, *et al.*), CLNS-94-1273, Feb 1994; submitted to *Phys. Rev. Lett.*

[7] Throughout this paper, charge conjugate states are implied.

[8] CLEO Collaboration (J. Gronberg *et al.*), contribution GLS0242 to this conference.

[9] CLEO Collaboration (R. Balest *et al.*), contribution GLS0455 to this conference.

[10] T. Das, V.S. Mathur and S. Okubo, *Phys. Rev. Lett.* **18**, 761 (1967).

[11] Particle Data Group, K. Hikasa *et al.*, *Phys. Rev.* **D45**, 1 (1992).

[12] M. Suzuki, *Phys. Rev.* **D47**, 1252 (1993); H.J. Lipkin, *Phys. Lett.* **B303**, 119 (1993); E.L. Berger and H.J. Lipkin, *Phys. Lett.* **B189**, 226 (1987).

[13] H.J. Lipkin, *Phys. Lett.* **B72**, 249 (1977).

[14] Y. Kubota *et al.*, Nucl. Instrum. Methods **A320**, 66 (1992).

[15] KORALB (v.2.1)/TAUOLA (v.1.5): S. Jadach and Z. Was, Comput. Phys. Commun. **36**, 191 (1985) and *ibid*, **64**, 267 (1991); S. Jadach, J.H. Kühn, and Z. Was, Comput. Phys. Commun. **64**, 275 (1991), *ibid*, **70**, 69 (1992), *ibid*, **76**, 361 (1993).

[16] R. Brun *et al.*, GEANT 3.15, CERN DD/EE/84-1.

[17] R. Decker, E. Mirkes, R. Sauer, and Z. Was, *Z. Phys.* **C58**, 445 (1993).

[18] CLEO Collaboration (M. Artuso *et al.*), *Phys. Rev. Lett.* **72**, 3762 (1994). Studies of the $\pi^{\pm}\pi^{0}$ invariant mass and decay angle distributions will be presented in a future publication.

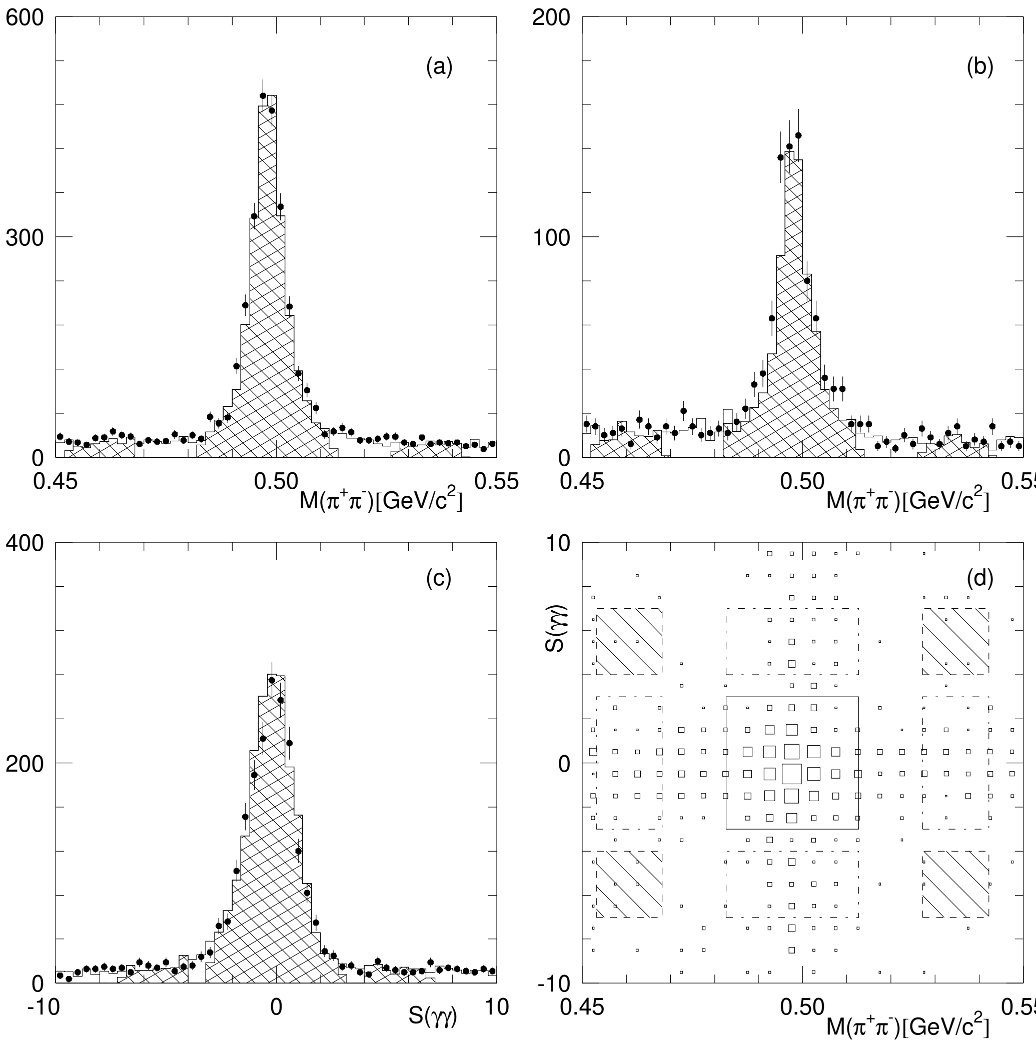

FIG. 1. The distributions of (a) $M_{\pi\pi}$ for the $K_S^0 h^-$ mode; and (b) $M_{\pi\pi}$, (c) $S_{\gamma\gamma}$, (d) $S_{\gamma\gamma}$ vs $M_{\pi\pi}$, for the $K_S^0 h^- \pi^0$ mode. Here, $S_{\gamma\gamma} \equiv (M_{\gamma\gamma} - M_{\pi^0})/\sigma_{\gamma\gamma}$. Points are data and histograms are $\tau^+\tau^-$ Monte Carlo. The 'signal' and 'sideband' regions are indicated as hatched regions.

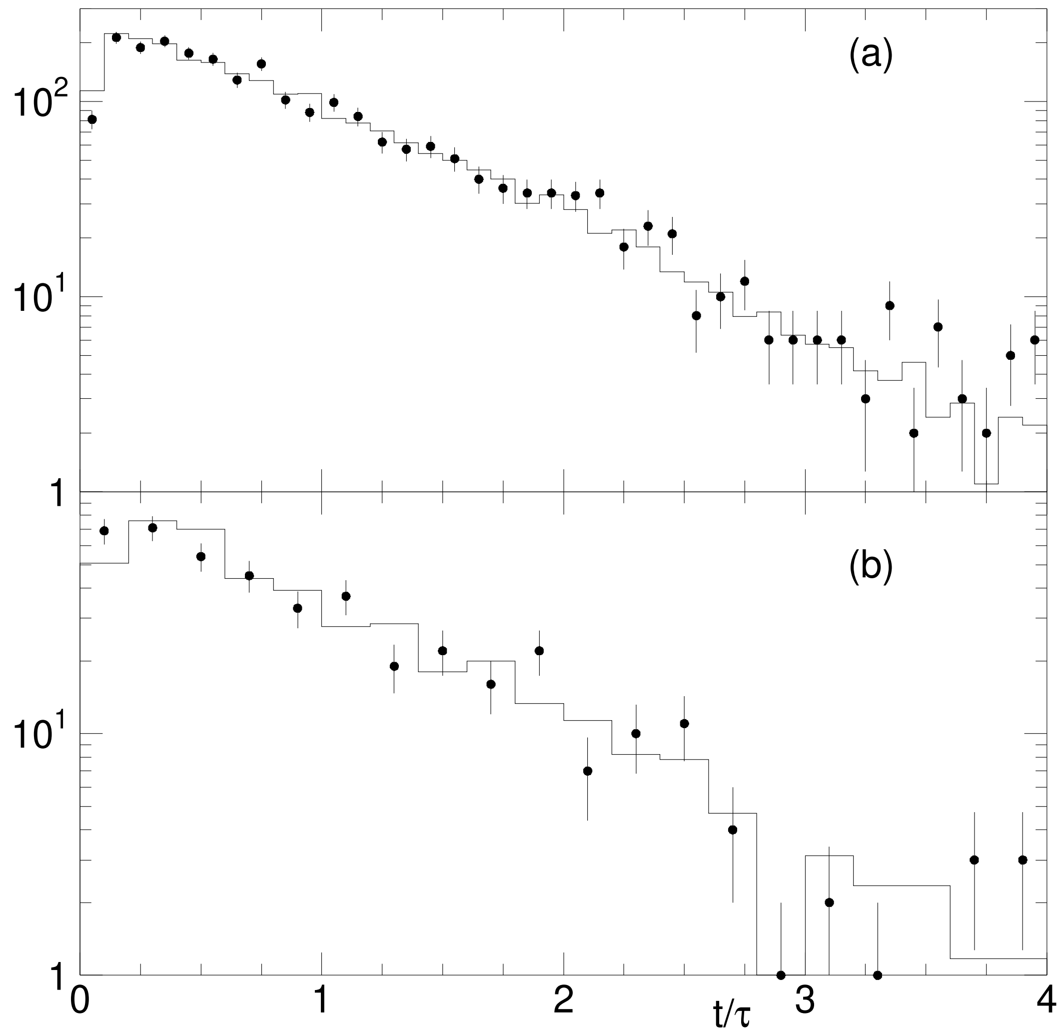

FIG. 2. The distribution of t/τ, the K_S^0 proper lifetime in units of its mean, for the (a) $K_S^0 h^-$ mode and (b) $K_S^0 h^- \pi^0$ mode. The histograms are signal MC, normalized to have the same area as data (points).

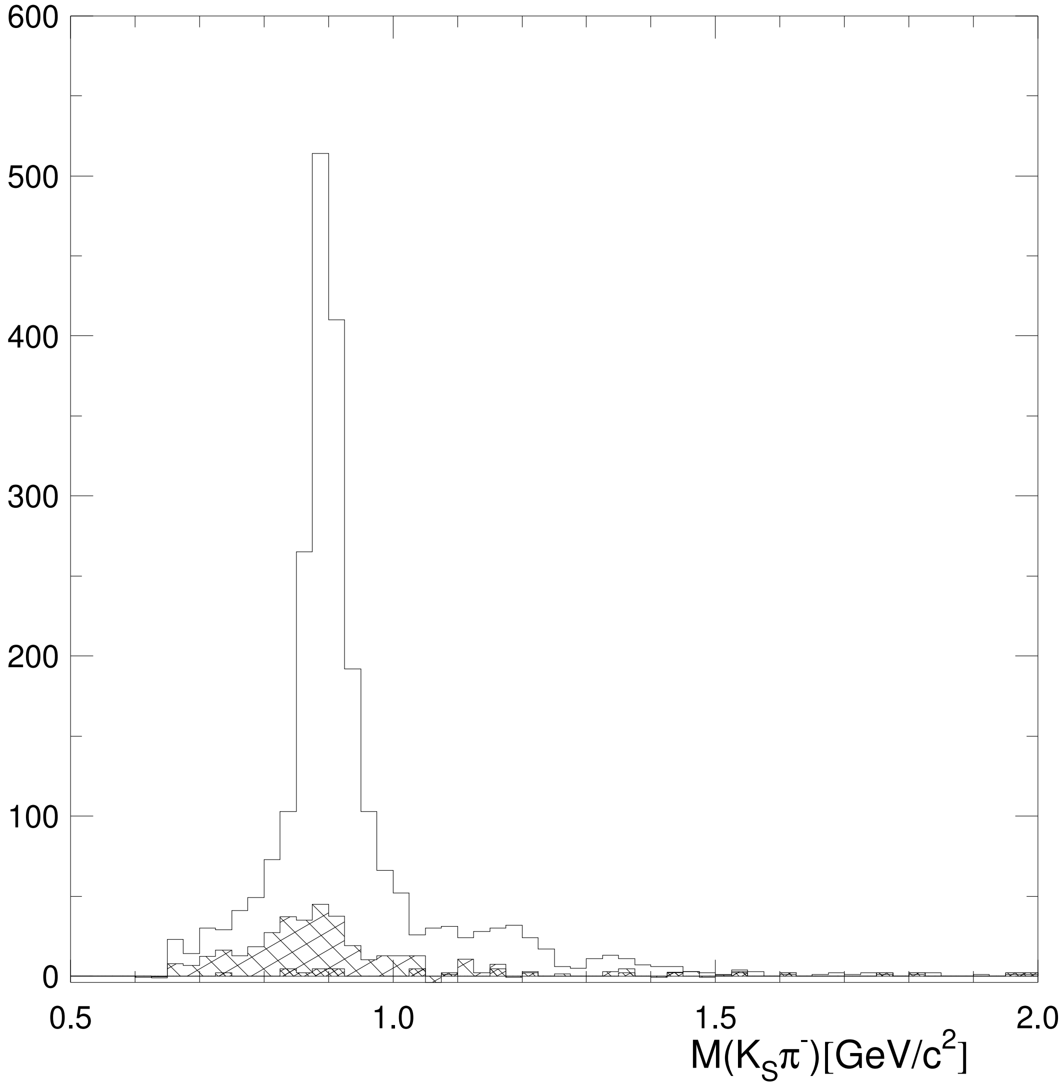

FIG. 3. The $M(K_S^0\pi^-)$ distribution, after the subtraction of sideband, for data (solid histogram) and the expected total background (lightly hatched histogram). The contribution from $q\overline{q}$ background is shown as the heavily hatched histogram.

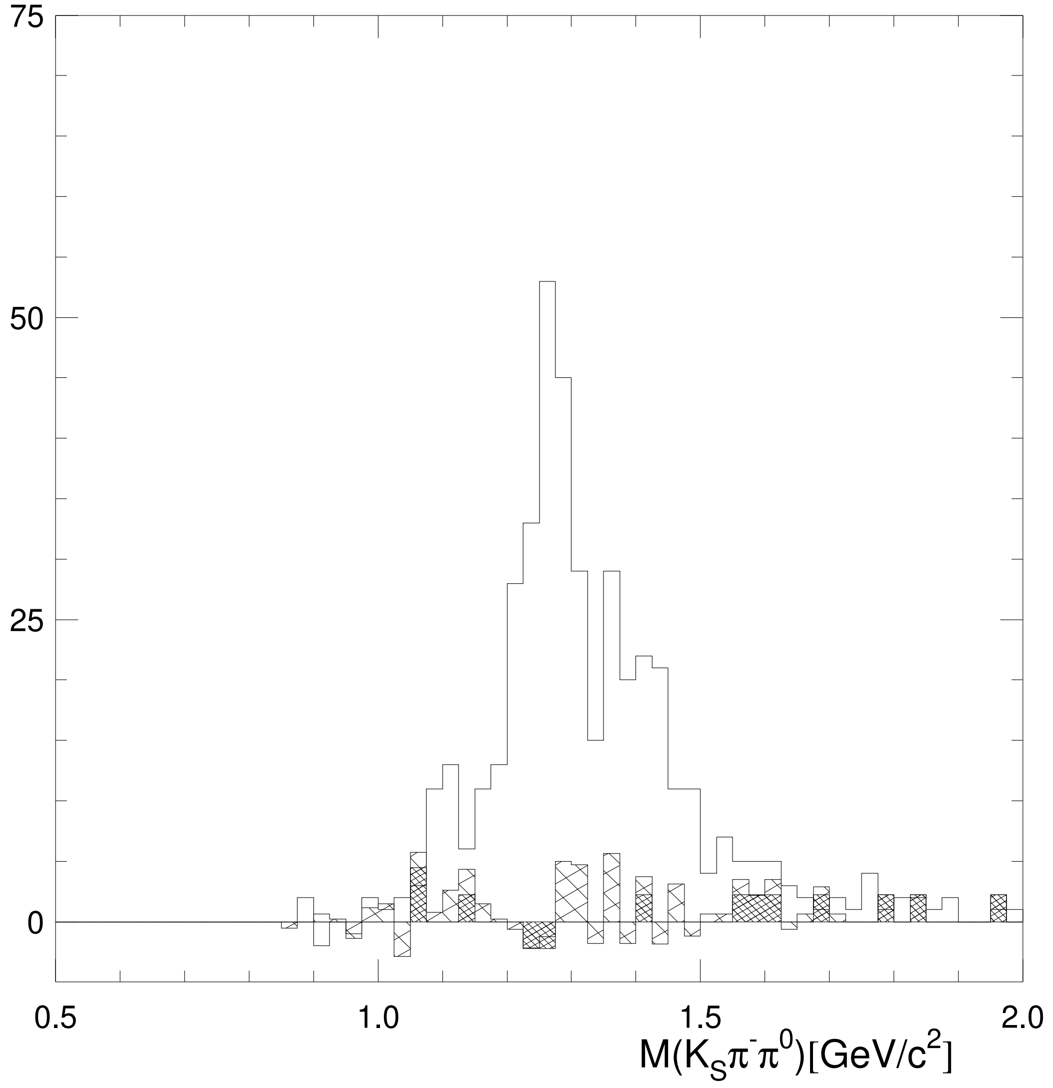

FIG. 4. The $M(K_S^0\pi^-\pi^0)$ distribution, after the subtraction of sideband, for data (solid histogram) and the expected total background (lightly hatched histogram). The contribution from $q\overline{q}$ background is shown as the heavily hatched histogram.

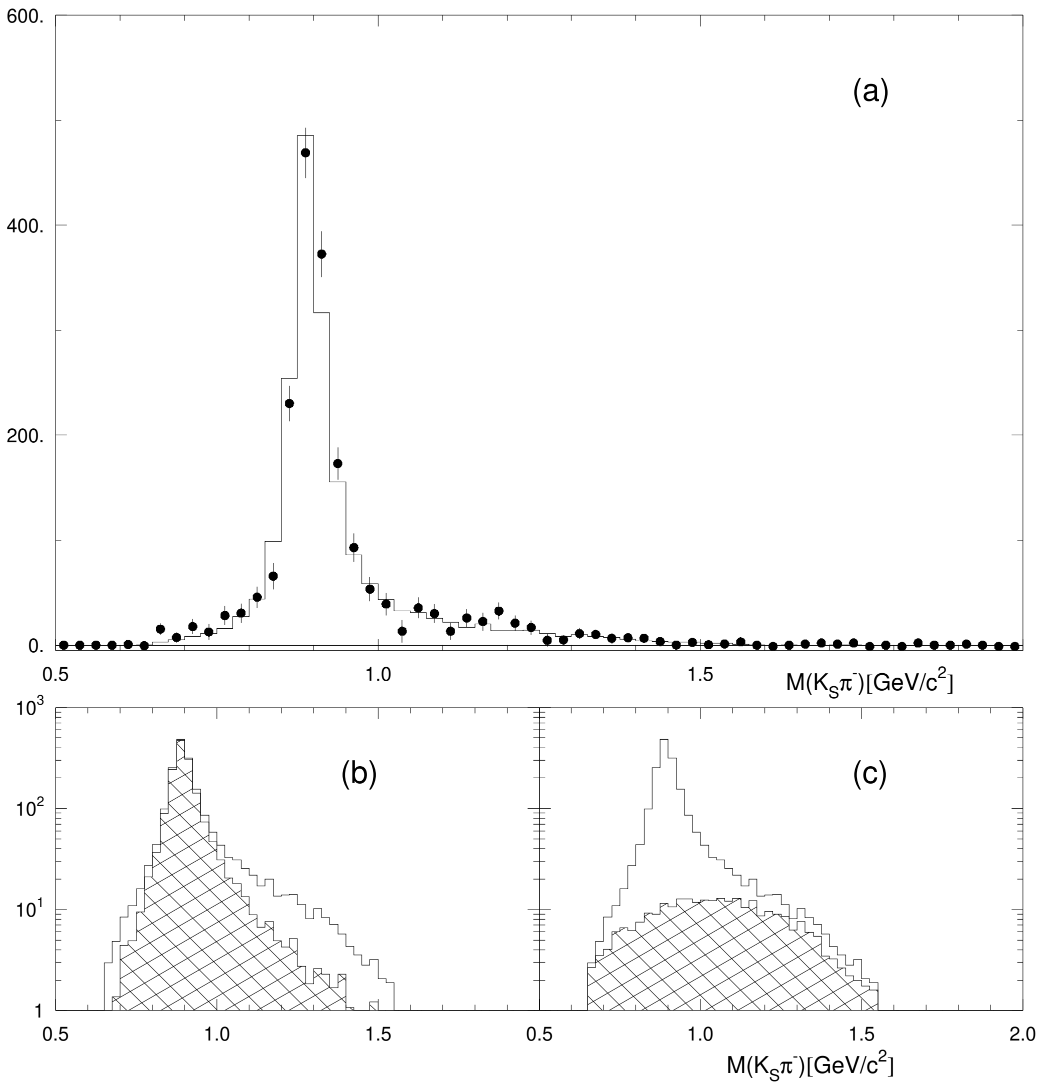

FIG. 5. (a) The $M(K_S^0\pi^-)$ distribution for data (points) after sideband and background subtraction. The solid histogram is the result of a fit to the Monte Carlo predicted distributions for $K^{*-} \to K_S^0\pi^-$, and a fixed contribution from $K_S^0K^-$ (according to the result in [8]). Their contributions are shown as hatched histograms in (b) and (c), respectively.

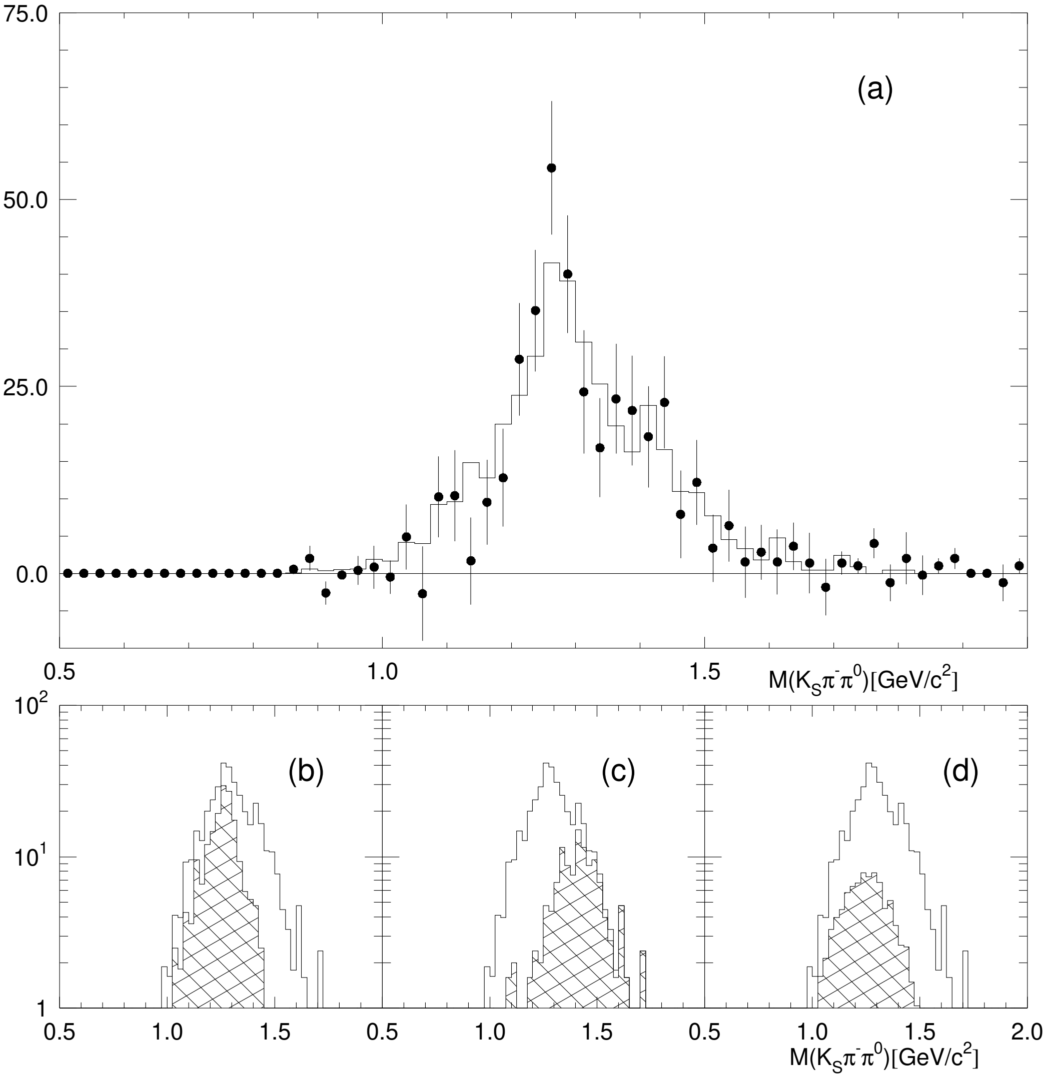

FIG. 6. (a) The $M(K_S^0\pi^-\pi^0)$ distribution for data (points) after sideband and background subtraction. The solid histogram is the result of a fit to the Monte Carlo predicted distributions for $K_1(1270)$ and $K_1(1400)$, and a fixed contribution from $K_S^0K^-\pi^0$ (according to the result in [8]). Their contributions are shown as hatched histograms in (b) ($K_1(1270)$), (c) ($K_1(1400)$) and (d) ($K_S^0K^-\pi^0$).

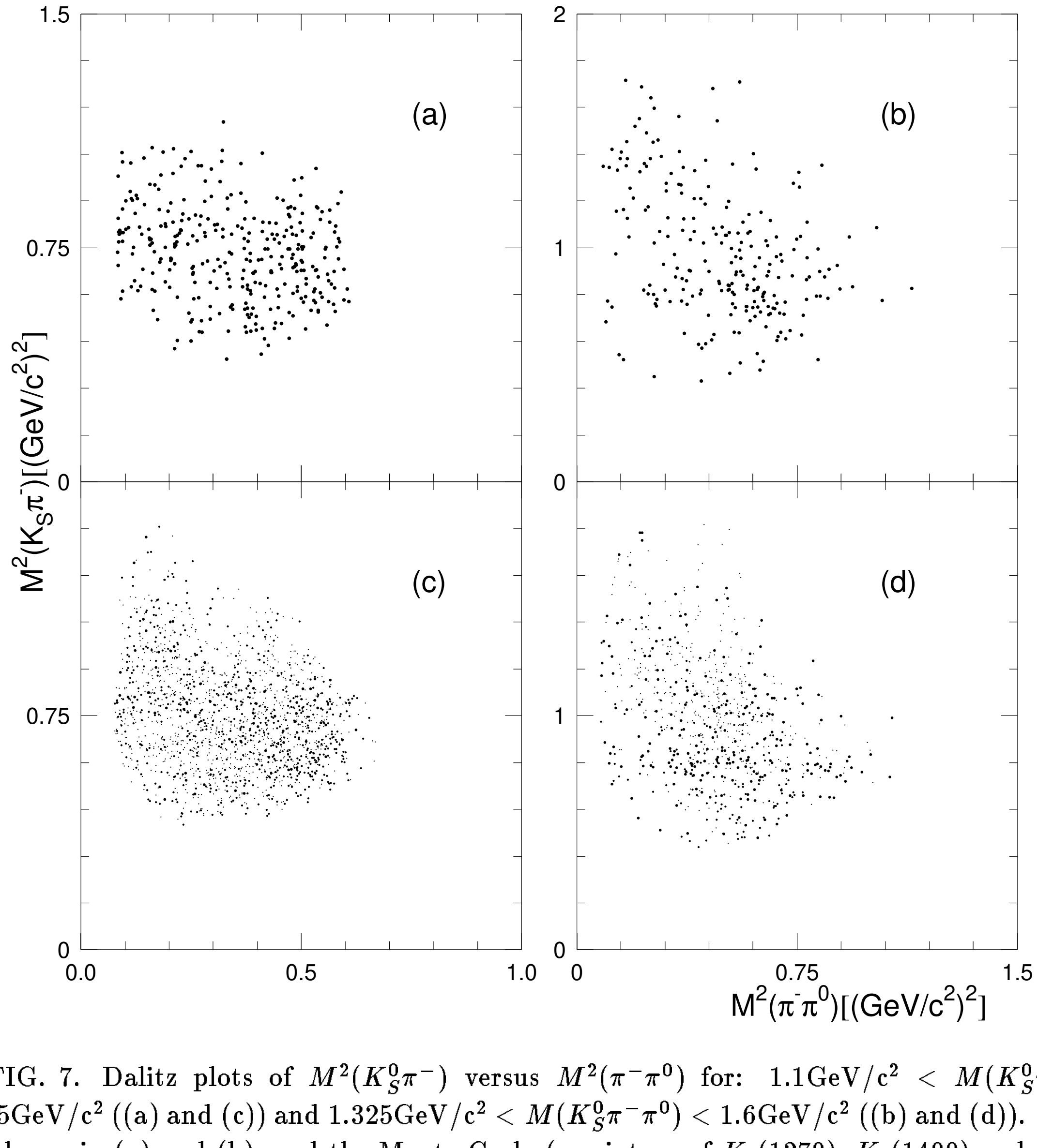

FIG. 7. Dalitz plots of $M^2(K_S^0\pi^-)$ versus $M^2(\pi^-\pi^0)$ for: $1.1\mathrm{GeV/c^2} < M(K_S^0\pi^-\pi^0) < 1.325\mathrm{GeV/c^2}$ ((a) and (c)) and $1.325\mathrm{GeV/c^2} < M(K_S^0\pi^-\pi^0) < 1.6\mathrm{GeV/c^2}$ ((b) and (d)). The data are shown in (a) and (b), and the Monte Carlo (a mixture of $K_1(1270)$, $K_1(1400)$ and $K_S^0K^-\pi^0$ according to the fit in Fig 6) predictions are shown in (c) and (d).